An in vivo selection-derived D-peptide for engineering erythrocyte-binding antigens that promote immune tolerance

Alexander R. Loftis[a,1], Genwei Zhang[a,1], Coralie Backlund[b], Anthony J. Quartararo[a], Novalia Pishesha[c,d], Cameron C. Hanna[a], Carly K. Schissel[a], Daniel Garafola[b], Andrei Loas[a], R. John Collier[e], Hidde Ploegh[c], Darrell J. Irvine[b,f,g,h,i], and Bradley L. Pentelute[a,b,d,j,2]

[a]Department of Chemistry, Massachusetts Institute of Technology, Cambridge, MA 02139; [b]Koch Institute for Integrative Cancer Research, Massachusetts Institute of Technology, Cambridge, MA 02142; [c]Program in Cellular and Molecular Medicine, Boston Children's Hospital, Boston, MA 02115; [d]Broad Institute of MIT and Harvard, Cambridge, MA 02142; [e]Department of Microbiology, Harvard Medical School, Boston, MA 02115; [f]Department of Biological Engineering, Massachusetts Institute of Technology, Cambridge, MA 02139; [g]Ragon Institute of Massachusetts General Hospital, Massachusetts Institute of Technology and Harvard University, Cambridge, MA 02139; [h]Department of Materials Science and Engineering, Massachusetts Institute of Technology, Cambridge, MA 02139; [i]Howard Hughes Medical Institute, Massachusetts Institute of Technology, Cambridge, MA 02139; and [j]Center for Environmental Health Sciences, Massachusetts Institute of Technology, Cambridge, MA 02139

Edited by James A. Wells, University of California, San Francisco, CA, and approved June 29, 2021 (received for review January 25, 2021)

When displayed on erythrocytes, peptides and proteins can drive antigen-specific immune tolerance. Here, we investigated a straightforward approach based on erythrocyte binding to promote antigen-specific tolerance to both peptides and proteins. We first identified a robust erythrocyte-binding ligand. A pool of one million fully D-chiral peptides was injected into mice, blood cells were isolated, and ligands enriched on these cells were identified using nano-liquid chromatography–tandem mass spectrometry. One round of selection yielded a murine erythrocyte-binding ligand with an 80 nM apparent dissociation constant, K_d. We modified an 83-kDa bacterial protein and a peptide antigen derived from ovalbumin (OVA) with the identified erythrocyte-binding ligand. An administration of the engineered bacterial protein led to decreased protein-specific antibodies in mice. Similarly, mice given the engineered OVA-derived peptide had decreased inflammatory anti-OVA CD8$^+$ T cell responses. These findings suggest that our tolerance-induction strategy is applicable to both peptide and protein antigens and that our in vivo selection strategy can be used for de novo discovery of robust erythrocyte-binding ligands.

in vivo selection | peptide libraries | immune tolerance | erythrocyte binders | antigens

As the principal cellular component of blood, erythrocytes not only play a critical role in the transport of oxygen but are also implicated in the induction of immune tolerance (1–4). In particular, covalent or noncovalent loading of antigens onto erythrocytes can drive antigen-specific tolerance, which mitigates antidrug antibody responses and other adverse inflammatory events. Still, the specific loading of peptide and protein antigens onto erythrocytes can be complex, requiring ex vivo manipulation or bioconjugation to an antibody (1, 2).

The conjugation of antigens to a peptide ligand is an attractive strategy for erythrocyte loading. Peptide ligands offer important advantages over other targeting ligand modalities (5, 6). Peptides can provide selective, high-affinity binding to a variety of molecular targets. Moreover, unlike larger biomolecules (e.g., antibodies), peptides are compatible with both organic solvents and aqueous conditions, thus allowing for a number of conjugation strategies. However, in general, the discovery of useful cell-binding peptides has been hindered by two factors—the proteolytic instability of L-peptides and the limitations inherent to the selection of cell-binding peptides in vitro. Unlike peptides composed of canonical L-amino acids, peptides synthesized from D-amino acids are not recognized by natural proteases and should thus be resistant to proteolysis (7–13). Consequently, ligand discovery techniques such as mirror image phage display have benefitted from their ability to generate D-peptide ligands (14, 15). In addition, in vitro selections of cell-binding ligands generally rely on tissue culture, which may not reflect the relevant form of the target cell or tissue. An in vivo selection, in contrast, ensures that identified ligands bind an accessible receptor in a physiologically relevant state (16).

Both limitations might be circumvented if a D-peptide library could be selected in vivo. Such a protocol might yield a high-affinity and stable ligand that reliably binds the target cell in vivo. To our knowledge, however, there are no ligand discovery protocols that enable the selection of D-peptide ligands in a living animal.

To investigate peptide and protein antigen-specific tolerance induction based on engineered erythrocyte binding, we first performed an in vivo D-peptide selection. This selection enabled the de novo discovery of a robust ligand that binds murine erythrocytes with high affinity. An administration of peptide and protein antigens modified with this ligand reduced the formation of antidrug antibodies and decreased inflammatory antigen-specific T cell responses.

Significance

Erythrocyte-bound antigens can drive immune tolerance in an antigen-specific fashion. Exploiting this phenomenon, we developed a general strategy to promote antigen-specific tolerance by engineering peptide and protein antigens to bind erythrocytes. Here, we showed that a fully D-chiral peptide library can be selected in vivo for the de novo discovery of a robust erythrocyte binder, which we attached to peptide and protein antigens. An administration of engineered peptide and protein antigens mitigated antigen-specific inflammatory responses, suggesting the generalizability of this immune tolerance-induction strategy and validating our in vivo ligand selection technique.

Author contributions: A.R.L., G.Z., C.B., A.J.Q., R.J.C., H.P., D.J.I., and B.L.P. designed research; A.R.L., G.Z., C.B., A.J.Q., N.P., C.C.H., C.K.S., and D.G. performed research; A.R.L., G.Z., C.B., A.J.Q., N.P., C.C.H., C.K.S., A.L., R.J.C., H.P., D.J.I., and B.L.P. analyzed data; and A.R.L., G.Z., A.L., and R.J.C. wrote the paper.

Competing interest statement: B.L.P. is a co-founder of Amide Technologies and Resolute Bio. Both companies focus on the development of protein and peptide therapeutics.

This article is a PNAS Direct Submission.

[1]A.R.L. and G.Z. contributed equally to this work.

[2]To whom correspondence may be addressed. Email: blp@mit.edu.

This article contains supporting information online at https://www.pnas.org/lookup/suppl/doi:10.1073/pnas.2101596118/-/DCSupplemental.

Published August 20, 2021.

Results

In Vivo Selection Yielded Multiple Putative Erythrocyte-Binding D-Peptide Ligands. To discover an erythrocyte-binding ligand, we performed a selection of a randomized D-peptide library in live mice (Fig. 1*A*). A 10^6-member 10-mer fully D-chiral peptide library with a design of X_9k (variable residues are listed in Fig. 1*A*) was prepared using split-and-pool peptide library synthesis. Library members were synthesized with C-terminal amides that enable distinction from endogenous peptides, which bear C-terminal carboxylic acids. This substitution results in a −0.98-Da mass difference relative to naturally occurring peptides, which can be reliably identified by mass spectrometry. Four mice were injected with amidated D-peptide library solution and then euthanized. Blood cells were isolated, and membrane-bound material was processed and prepared for mass spectrometry (see *Methods* for details). Nano-liquid chromatography–tandem mass spectrometry (nLC-MS/MS) identified 128 putative blood-binding amidated 10-mer D-peptide ligands. A positional frequency analysis indicated a preference among these hits for a D-phenylalanine at P1 and D-tryptophan at P2 (Fig. 1*B*). The strongest amino acid preference was for D-proline at P4, which occurred in over half of library sequences identified from our randomized peptide library.

Consensus-Derived D-Peptide Ligands Bind Erythrocytes with Varying Affinities. Based on our initial results, we synthesized a set of individual peptides with varying resemblance to the consensus motif (Fig. 2*A*). We reasoned that, because of their abundance, erythrocytes were the likely binding partner in a blood-based affinity selection. We therefore used flow cytometry on mouse erythrocytes to determine the apparent binding constants of Alexa Fluor 488–labeled versions of these peptides (Fig. 2*B* and *SI Appendix*, Fig. S1). Peptides with the highest affinity generally resembled the consensus motif. In particular, peptides with the consensus D-proline at P4 had measurable affinity for erythrocytes, and those that lacked a P4 D-proline did not. The peptide with the highest affinity, referred to hereafter as DQLR, contained the consensus P1 D-phenylalanine, consensus P2 D-tryptophan, and consensus P4 D-proline. In line with these observations, N-terminal truncations of DQLR dramatically reduced the binding affinity to erythrocytes, whereas C-terminal truncations had a more modest effect (*SI Appendix*, Fig. S2).

DQLR Is a Sequence-Specific Mouse Erythrocyte Binder. We prepared conjugates of DQLR with green fluorescent protein (GFP) and Alexa Fluor 488 fluorophore and found that both constructs retained affinity for mouse erythrocytes (Fig. 2*C*). DQLR–Alexa Fluor 488 bound with an 80-nM apparent dissociation constant, while DQLR-GFP had a 370-nM apparent dissociation constant. Neither a scrambled sequence of the DQLR peptide nor the L-enantiomer of DQLR had measurable affinity for erythrocytes. These findings suggest that the association of DQLR to erythrocytes is driven by the DQLR amino acid sequence and not by the reporter molecules used for detection. We conclude that DQLR binding involves molecular recognition as opposed to nonspecific interactions.

We compared the binding of GFP and DQLR-GFP to mouse erythrocytes and leukocytes (Fig. 2*D*). GFP and DQLR-GFP displayed similar binding to splenic leukocytes, at 1 μM concentration, barely detectable above the intrinsic fluorescence of leukocytes alone. In contrast, DQLR-GFP bound to erythrocytes with a signal well above background levels of autofluorescence, whereas GFP did not. This line of evidence suggests that DQLR binds erythrocytes selectively and does not enhance the weak association of GFP with leukocytes.

We performed an unbiased photoaffinity labeling experiment on erythrocytes to determine the molecular basis for this selectivity. Using a diazirine-modified and biotinylated DQLR probe, we identified that the putative DQLR receptor is the transmembrane protein Band 3, which is a major integral protein of the erythrocyte membrane (*SI Appendix*, Fig. S3). This finding aligns with the robust binding of DQLR to erythrocytes and lack of affinity for splenic leukocytes.

Based on these results, we further probed DQLR's cell selectivity. We characterized the binding of DQLR to mouse M-1 cells, which generally display characteristics of principal cells or kidney-collecting duct intercalated cells, a subset of which are known to express an isoform of Band 3 (17, 18). Biotinylated DQLR was incubated with M-1 cells or B16F10 cells, a control cell line which is not known to express Band 3. Binding was detected using a streptavidin fluorophore (*SI Appendix*, Fig. S4). DQLR was observed to bind M-1 at micromolar concentrations and was not observed to bind B16F10 at any concentration

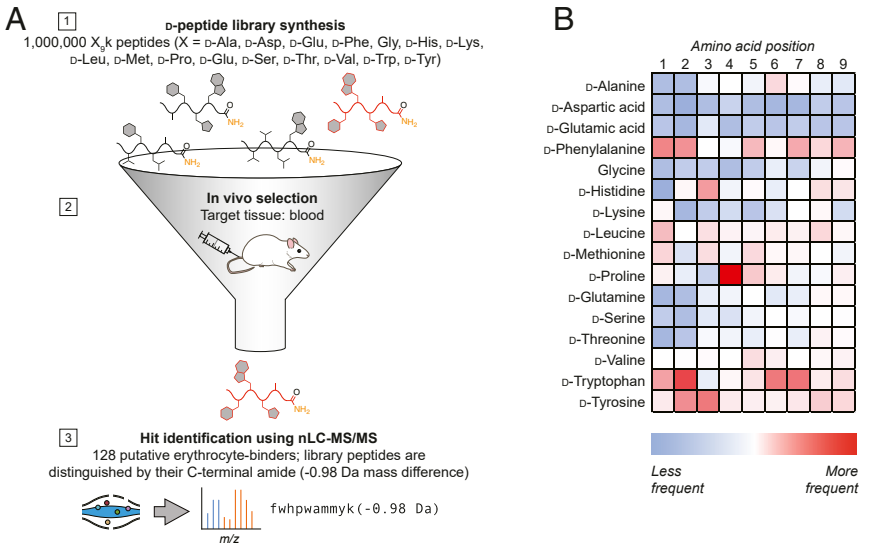

Fig. 1. In vivo selection of a D-peptide library enables de novo discovery of 128 putative erythrocyte binders. (*A*) Description of our three-step in vivo selection strategy to discover tissue-targeting peptides from a randomized 10^6-member D-peptide library. (*B*) Positional frequency analysis of identified sequences indicates a preference for first-position D-phenylalanine, second position D-tryptophan, and fourth position D-proline.

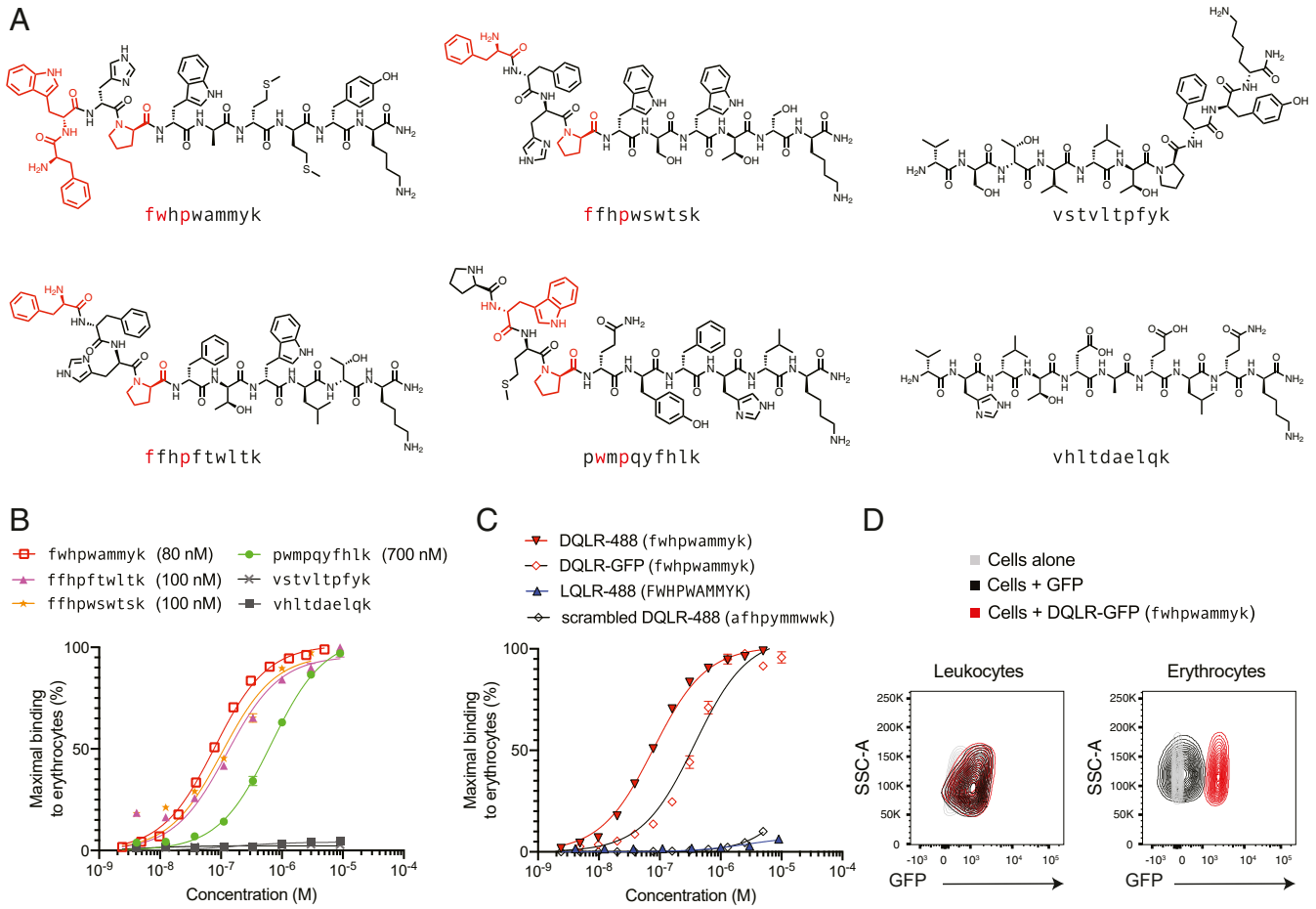

Fig. 2. Analysis of hits from in vivo selection uncovers a high-affinity erythrocyte-binding D-peptide. (*A*) Structures of select hits identified from the in vivo selection. Red indicates a residue which matches the consensus motif. (*B*) Select Alexa Fluor 488–labeled hits bind mouse erythrocytes with varying affinities (apparent dissociation constant, K_d, in parentheses) as determined by flow cytometry ($n = 3$; data presented as mean ± SEM). (*C*) Alexa Fluor 488–labeled DQLR and GFP-labeled DQLR bind mouse erythrocytes, whereas scrambled DQLR and the L-enantiomer of DQLR do not as determined by flow cytometry ($n = 3$; data presented as mean ± SEM). (*D*) GFP-labeled DQLR binds specifically to erythrocytes and not to splenic leukocytes as determined by flow cytometry.

tested. This result indicates that, in vivo, DQLR may also bind intercalated cells via Band 3.

We also assessed DQLR's ability to bind human erythrocytes. Biotinylated DQLR was incubated with human red blood cells (hRBCs) at varying concentrations of peptide and then detected using a streptavidin fluorophore (*SI Appendix*, Fig. S5). At micromolar concentrations, DQLR was observed to bind hRBCs, therefore demonstrating cross-reactivity.

Conjugation of DQLR to a Bacterial Protein Decreased Antibody Responses to the Protein in Mice. We investigated the ability of DQLR to direct an 83-kDa protein antigen to erythrocytes and mitigate an antibody response to the protein. Protective antigen (PA), a nontoxic protein antigen derived from anthrax toxin, is both immunogenic and of therapeutic interest (19–25). We prepared a mutant form of PA, mPA (K563C, N682A, D683A), and labeled it with DQLR and biotin. Biotinylated DQLR-mPA was prepared with a peptide:protein ratio ranging from 0:1 to 2:1 as determined by LC-MS (Fig. 3*A*; median of 1:1 labeling). We similarly prepared an mPA construct labeled with scrambled DQLR. DQLR-mPA bound to erythrocytes, whereas scrambled DQLR-mPA did not (Fig. 3*B*).

Mice were given either wild-type antigen PA or erythrocyte-binding antigen DQLR-mPA and then challenged with PA (Fig. 3*C*). Anti-PA antibody titers determined before and after the challenge showed a durable, significant decrease in the anti-PA antibody response in the DQLR-mPA group. An administration of scrambled DQLR-mPA or a mixture of DQLR peptide and PA did not significantly decrease the anti-PA response as compared to animals that received only PA, indicating that the decrease in response depends on covalent linkage of DQLR to mPA (Fig. 3*D*). Additionally, we infer that the modification of PA with an irrelevant D-peptide is not sufficient for the induction of tolerance, and DQLR alone does not exhibit immunosuppressive properties. Taken together, these results suggest that the physical association of an engineered protein antigen with erythrocytes mediated by the erythrocyte-binding ligand DQLR has an antigen-specific tolerogenic effect.

DQLR-SIINFEKL Conjugate Decreases OVA-Specific T Cell Responses in Mice. We next investigated the immune response to a peptide antigen engineered to bind erythrocytes. We synthesized a DQLR-SIINFEKL peptide composed of DQLR linked to the peptide SIINFEKL, derived from a full-length ovalbumin (OVA) protein (Fig. 4*A*). Mice received Thy1.1$^+$ CD8$^+$ T cells from T cell receptor (TCR) transgenic OT1 mice. These transgenic T cells have TCRs that are specific for SIINFEKL-loaded H-2K^b complexes. Mice were then given either a DQLR-SIINFEKL peptide or SIINFEKL peptide alone (Fig. 4*B*). Mice were then challenged via intradermal injection of full-length OVA and lipopolysaccharide (LPS). In a "naïve" control group, mice received OT1 T cells, did not receive the OVA challenge, and were given phosphate-buffered

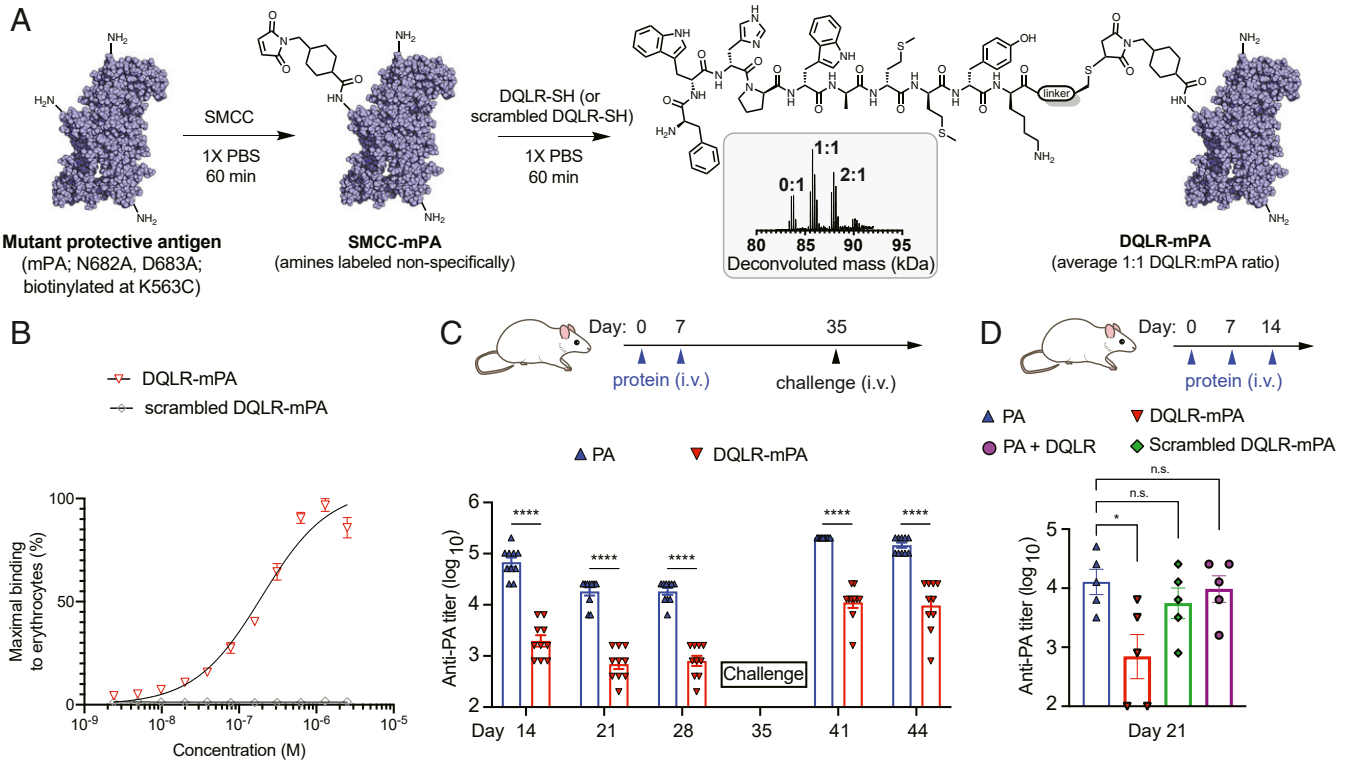

Fig. 3. Administration of an erythrocyte-binding DQLR mutant PA conjugate decreases protective antigen-specific antibody formation. (*A*) Synthesis and LC-MS characterization (*Inset*) of DQLR-labeled mPA (K563C, N682A, D683A; DQLR-mPA). Peptide-to-protein ratios are indicated in the LC-MS *Inset* in parentheses. (*B*) DQLR-mPA binds to mouse erythrocytes, whereas scrambled DQLR-mPA does not as determined by flow cytometry ($n = 3$; data presented as mean ± SEM). (*C*) BALB/c mice have decreased anti-PA antibody responses as a result of injection of DQLR-mPA as compared to PA, even following a PA challenge to both groups ($n = 10$; data presented as mean ± SEM; $^{****}P < 0.0001$, one-way ANOVA with a Sidak's multiple comparisons test). (*D*) A decreased response is not observed when PA and DQLR are administered separately or when scrambled DQLR-mPA is administered ($n = 5$; data presented as mean ± SEM; $^{*}P < 0.05$, one-way ANOVA with a Dunnett's multiple comparisons test; n.s., not statistically significant).

saline (PBS) instead of peptides. In a challenge group that served as a further control, mice received OT1 T cells and the OVA challenge but were similarly given PBS instead of peptides. On day 19, peripheral blood leukocytes were stimulated ex vivo with a SIINFEKL peptide, and the percentage of $CD8^+$ T cells producing intracellular interferon-gamma (IFN-γ^+) was determined by flow cytometry. On day 21, draining inguinal lymph nodes were harvested, and the percentage of Thy1.1$^+$ $CD8^+$ T cells was determined. Compared to mice that received a SIINFEKL peptide alone, mice that received DQLR-SIINFEKL had significantly fewer IFN-γ^+ $CD8^+$ T cells and SIINFEKL-H-2K^b–reactive OT1 $CD8^+$ T cells (Fig. 4 *C* and *D* and *SI Appendix*, Figs. S6 and S7). Taken together, these results suggest that the engineered DQLR-SIINFEKL peptide drove the deletion of the OT1 T cell population and generated an anti-inflammatory response. Under these experimental conditions, a conjugate of SIINFEKL to a previously reported erythrocyte-binding L-peptide (ERY1-SIINFEKL) did not significantly reduce the level of IFN-γ^+ $CD8^+$ T cells or OT1 $CD8^+$ T cells as compared to SIINFEKL alone (*SI Appendix*, Fig. S8). These outcomes validate our peptide engineering approach for antigen-specific tolerance induction as well as our in vivo selection strategy for de novo discovery of erythrocyte-binding D-peptides.

Discussion

Erythrocytes have gained attention for their role in establishing tolerance. Recent work suggests that antigens displayed on the surface of erythrocytes can drive antigen-specific tolerance (1–3, 26, 27). We sought to identify an erythrocyte-binding D-peptide to explore the generalizability of this phenomenon. In particular, we hypothesized that a variety of antigens could be attached to a stable, high-affinity D-peptide ligand to induce antigen-specific tolerance. Indeed, DQLR mediates association of other molecules to erythrocytes. Consistent with a model of erythrocyte-driven antigen presentation and induction of tolerance, the administration of an engineered DQLR-mPA protein antigen decreased the formation of antibodies against PA. Similarly, upon the administration of an engineered DQLR-SIINFEKL peptide antigen, we saw a decrease in the SIINFEKL-specific inflammatory T cell response and OT1 T cell population. Importantly, DQLR can be attached to payloads using multiple conjugation routes—in these studies alone, we employed sortase-mediated ligation, thiol-maleimide conjugation, and solid-phase peptide synthesis to install DQLR. Looking forward, engineered DQLR peptide and DQLR protein antigens merit further investigation as a possible therapy for inflammatory or autoimmune disorders. DQLR antigens might likewise be administered prophylactically to enable the use of therapeutics that are hindered by their immunogenicity.

In general, erythrocyte-targeted antigens have demonstrated variable effects on humoral response. No tolerogenic effects were observed in the initial characterization of the L-peptide ERY1 (26), but a significantly enhanced response was observed in later studies (3). The responses observed here lie somewhere in the middle, even though a direct comparison across the studies is not feasible. Further study of DQLR antigens and other erythrocyte-targeted antigens is needed to understand the factors that determine a meaningful reduction in antigen-specific antibodies. Binding affinity to erythrocytes, receptor identity, and the native antigen's immunogenicity are all likely to play a role.

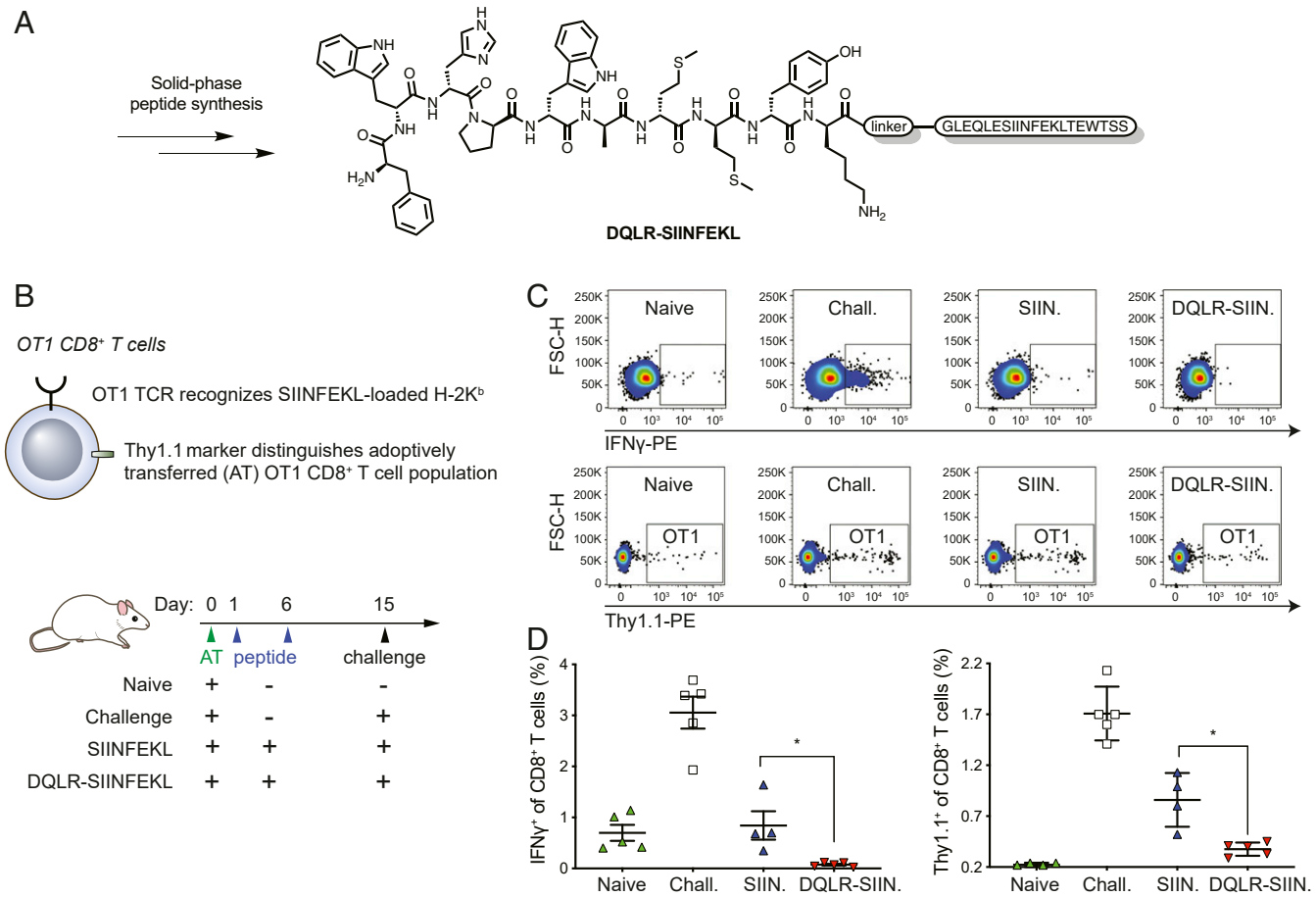

Fig. 4. Administration of an erythrocyte-binding DQLR-SIINFEKL antigen promotes OVA-specific anti-inflammatory T cell responses in an OT1 mouse model. (*A*) Structure of DQLR-SIINFEKL peptide, which is prepared by solid-phase peptide synthesis. SIINFEKL is a peptide derived from full-length OVA protein. (*B*) Diagram and injection scheme to determine OVA-specific antigen response following administration of DQLR-SIINFEKL peptide, SIINFEKL peptide, or controls. (*C* and *D*) Mice administered DQLR-SIINFEKL have decreased proinflammatory T cell responses to SIINFEKL as determined by ex vivo SIINFEKL stimulation of peripheral blood-derived IFN-γ$^+$ CD8$^+$ T cells and measurement of draining inguinal lymph node–derived SIINFEKL-H-2K^b–reactive OT1 CD8$^+$ T cells ($n = 4$ for SIINFEKL group, $n = 5$ for other groups; data presented as mean ± SEM; $^*P < 0.05$, Mann–Whitney *U* test).

Our ligand discovery approach allows users to perform selections in vivo using a D-peptide library. Hits identified on the target cell type or tissue are likely to be effective targeting ligands, for multiple reasons. Inasmuch as the D-peptides are intrinsically stable to proteolysis, no additional steps are needed to enhance stability (14). Moreover, ligands discovered from an in vivo selection necessarily bind the target in its physiologic state at detectable quantities (16). Finally, this is both an "in solution" and "label-free" selection technique in which peptide library members are unencumbered by display scaffolds or encoding tags (28, 29). Techniques such as messenger RNA display, one-bead one-compound, and phage display, in contrast, must install a significant modification on each library member. In this regard, our technique offers superior fidelity. We envision that this strategy could be used to discover synthetic ligands that recognize targets beyond erythrocytes, including specific cells, tissues, and organs of therapeutic interest. Because this technique is compatible with chemically synthesized libraries, we also believe this method could be used to investigate structure–function relationships between the properties of synthetic peptides (e.g., stereochemistry, noncanonical functional groups, synthetic peptide structures, and supramolecular configurations) and the complex biological and physical features in animal models.

While our strategy offers unique advantages, we acknowledge its limitations. In this approach, cell-binding ligands are selected in vivo in a receptor-agnostic manner. Therefore, this method is applicable when the "target" is a cell type and less applicable when the "target" is a specific protein. This feature differentiates our method from others which employ isolated recombinant proteins. Moreover, to be clinically useful, ligands identified using our method must be cross-reactive in humans. DQLR binds both mouse and hRBCs. However, it is unlikely that every ligand identified with this method will have cross-reactivity, which will vary based on species-to-species homology and expression of receptors. Finally, while not unique to our strategy, ligands identified from our selections may have receptors that are expressed on off-target cells, which may result in off-target binding. An isoform of Band 3 is expressed on both erythrocytes and kidney-collecting duct intercalated cells, and DQLR binds both cell types. Importantly, this off-target binding did not prevent DQLR antigens from inducing antigen-specific tolerance.

Methods

Peptide Synthesis and Purification.

Peptide synthesis. Automated fast-flow synthesis of peptide-$^\alpha$carboxamides, as previously described (30–32), was carried out using H-Rink Amide-ChemMatrix resin (0.45 mmol/g, 0.1 mmol scale) at 90 °C. For manual, batch amino acid coupling and modification, fritted syringes (Torviq)

containing peptide resin were washed with *N,N*-dimethylformamide (DMF). Fmoc-protected amino acids (5 eq) in 1-[Bis(dimethylamino)methylene]-1*H*-1,2,3-triazolo[4,5-*b*]pyridinium 3-oxide hexafluorophosphate (HATU) solution (0.38 M, 4.5 eq) were activated with *N,N*-diisopropylethylamine (DIEA) (15 eq) and added to the resin bed. Resin was incubated at room temperature for 20 min and then washed three times with DMF. The Fmoc-protecting group was removed using 20% piperidine in DMF. The SIINFEKL peptide (sequence: GLEQLESIINFEKLTEWTSS) used in the OT1 experiment and for ex vivo stimulation was purchased from Genscript.

Library synthesis. The split-and-pool synthesis of the peptide library was carried out on 130-μm TentaGel resin (0.26 mmol/g). Splits were performed in 18 plastic fritted syringes on a manifold. Couplings were carried out using solutions of Fmoc-protected amino acids, HATU (0.38 M in DMF; 0.9 eq relative to amino acid), and DIEA (1.1 eq for histidine; 3 eq for all other amino acids). Resin was incubated at room temperature for 20 min and then washed three times with DMF. The Fmoc-protecting group was removed using 20% piperidine in DMF. Resin was washed again with DMF.

Peptide cleavage and purification. Peptide cleavage from solid support and global deprotection was carried out by adding a solution of 94% (vol/vol) trifluoroacetic acid (TFA), 2.5% (vol/vol) ethanedithiol, 2.5% (vol/vol) water, and 1.0% (vol/vol) triisopropylsilane to resin and incubating at room temperature for 2 h. The peptide was precipitated and triturated three times using diethyl ether. The crude peptide was dissolved in 50/50 water/acetonitrile (0.1% TFA) and lyophilized. Peptides were purified by mass-directed semipreparative reversed-phase high-performance liquid chromatography (HPLC; Agilent). Solvent A was water with 0.1% TFA, and solvent B was acetonitrile with 0.1% TFA. Peptides were generally purified with a 0.5% B/min gradient on a C3 SB Zorbax column (9.4 × 250 mm, 5 μm). Fractions were analyzed by LC-MS, and the purest fractions were pooled.

In Vivo Selection. Library stock solution (7.4 mM) in PBS was filtered using a 0.2 μm SPIN-X filter (Corning), and pH was adjusted to 7.0. Library solution was administered by tail vein to C57BL/6J mice (Taconic). Mice were female and 27 wk old. The exact volume administered was 170 to 200 μL. After 10 min, mice were euthanized by asphyxiation. Subsequently, a cardiac puncture was performed to retrieve as much blood as possible, and blood was collected into labeled ethylenediaminetetraacetic acid (EDTA)-coated collection vials. The exact quantity of blood collected was 400 to 600 μL. Vials were stored on ice for roughly 30 min before tissue processing. For processing, blood samples (from in vivo selection) were transferred to 1.6-mL microcentrifuge tubes. Blood was washed once with PBS and then centrifuged at 500 *g* for 3 min. Blood was then washed with RBC Lysis Buffer (Stem Cell Technologies) and then centrifuged at 16,000 *g* for 10 min. This was repeated twice. The cell pellet was resuspended in 50/50 water/acetonitrile (0.1% TFA), incubated at room temperature for 10 min, and then centrifuged at 16,000 *g* for 10 min. The supernatant was transferred to a new microcentrifuge tube and lyophilized overnight. The lyophilized material was resuspended in 95/5 water/acetonitrile (0.1% TFA) containing 6 M guanidine hydrochloride. The suspension was centrifuged at 16,000 *g* for 10 min, and the supernatant was transferred to a new microcentrifuge tube. This was repeated until the pellet formed by centrifugation was no longer visible (~10 rounds of centrifugation). The final supernatant was purified by solid-phase extraction using a 100-μL bed C18 tip according to the manufacturer's protocol (Pierce). The eluate was lyophilized in a 200-μL strip tube overnight. The lyophilized material was resuspended in water (0.1% TFA) and centrifuged at 16,000 *g* for 5 min. The supernatant was analyzed by nLC-MS/MS.

Preparation of Proteins and Protein Conjugates.

GFP. *E. coli*–expressing G3-GFP were grown at 37 °C in Luria Bertani (LB) broth to an optical density ($OD_{600\ nm}$, measured at a wavelength of 600 nm) of 0.6 and then grown overnight at 30 °C. Bacteria were centrifuged at 8,000 *g* at 4 °C and stored at −80 °C overnight. The following day, pellets were thawed on ice and homogenized by magnetic stirring and using a sonication probe (Branson). The lysate was centrifuged at 8,000 *g* at 4 °C, and the supernatant was purified using an AKTA Pure FPLC equipped with a HisTrap FF crude 5-mL column (GE Healthcare). Solvent A was 20 mM Tris pH 7.5. Solvent B was 20 mM Tris and 300 mM imidazole, pH 7.5. The gradient used was 0 to 50% B over 20 column volumes. The fraction purity was assessed by sodium dodecyl sulfate–polyacrylamide gel electrophoresis (SDS-PAGE). The purest fractions were collected, filtered using a 0.2-μm filter, snap frozen in liquid nitrogen, and stored at −80 °C.

PA and mPA. *E. coli* pellets containing periplasm-localized wild-type PA and mPA (K563C, N682A, D683A) were obtained from a protein expression facility and purified using an osmotic shock method. A pellet was thawed in sucrose buffer (20% sucrose [wt/vol], 20 mM Tris, and 1 mM EDTA, pH 8.0) and homogenized by magnetic stirring at 4 °C. The cell homogenate was centrifuged at 8,000 *g* for 20 min at 4 °C. The supernatant was discarded, and the pellet was resuspended in 5 mM magnesium sulfate buffer and homogenized. The homogenate was stirred for 30 min at 4 °C. The homogenate was centrifuged as before, and the supernatant was purified on an AKTA Pure FPLC equipped with a HiTrap Q 5-mL anion exchange column (GE Healthcare). Solvent A was 20 mM Tris, pH 8.5. Solvent B was 20 mM Tris and 1 M sodium chloride, pH 8.5. The gradient used was 0 to 25% B over 11 column volumes. The fraction purity was assessed by SDS-PAGE. The purest fractions were collected. These were further purified by size exclusion chromatography on a HiLoad 26/600 Superdex 200-pg column using an isocratic 1.5 column volume elution employing 20 mM Tris and 150 mM sodium chloride, pH 7.5 buffer. The purest fractions, as determined by SDS-PAGE, were filtered using a 0.2-μm filter, snap frozen in liquid nitrogen, and stored at −80 °C.

DQLR-mPA and scrambled DQLR-mPA. mPA (K563C, N682A, D683A) was modified with 10 equivalents of biotin-maleimide (Sigma Aldrich) at room temperature for 30 min. This biotin was installed for flow cytometry–based binding experiments using streptavidin phycoerythrin. Biotinylated mPA was then modified with 10 equivalents of sulfosuccinimidyl 4-(*N*-maleimidomethyl) cyclohexane-1-carboxylate (sulfo-SMCC; Thermo Fisher Scientific) at room temperature for 1 h. Finally, SMCC-modified biotinylated mPA was modified with 10 equivalents of DQLR-SH or scrambled DQLR-SH at room temperature for 1 h. After each reaction, protein was buffer exchanged three times into new buffer to remove unreacted small molecules and peptides. The final protein–peptide conjugates were filtered using 0.2-μm filters, snap frozen in liquid nitrogen, and stored at −80 °C.

DQLR-GFP. DQLR-LPXTG (1 mM) was enzymatically ligated to G3-GFP (100 μM) using pentamutant sortase (33) (5 μM) in sortase buffer (10 mM calcium chloride, 20 mM Tris, and 150 mM sodium chloride, pH 7.5) at room temperature for 1 h. The reaction product was then purified on an AKTA Pure FPLC equipped with a HiLoad 26/600 Superdex 200-pg column using an isocratic 1.5 column volume elution employing 20 mM Tris and 150 mM sodium chloride, pH 7.5 buffer. The pure fractions, as determined by SDS-PAGE, were filtered using a 0.2-μm filter, snap frozen in liquid nitrogen, and stored at −80 °C.

MS. LC-MS was performed on a 6520 Electrospray Ionization Quadrupole Time-of-Flight LC-MS (Agilent) equipped with an Agilent C3 Zorbax column (300SB C3, 2.1 × 150 mm, 5 μm). Solvent A was water with 0.1% formic acid (FA), and solvent B was acetonitrile with 0.1% FA. The method used was 1% B for 2 min, 1 to 61% B over 9 min, 61 to 99% B over 1 min, and 3 min post-time at 1% B. Data were processed using Agilent MassHunter.

nLC-MS/MS was performed on an EASY-nLC 1200 (Thermo Fisher Scientific) liquid chromatography system equipped with a PepMap RSLC C18 column (15 cm × 50 μm, 2 μm; Thermo Fisher Scientific) and a C18 nanoViper Trap Column (20 mm × 75 μm, 3 μm, 100 Å; Thermo Fisher Scientific) connected to an Orbitrap Fusion Lumos Tribrid Mass Spectrometer (Thermo Fisher Scientific). Solvent A was water (0.1% FA), and solvent B was 80% acetonitrile, 20% water (0.1% FA). The nLC gradient was 1% solvent B in solvent A ramping linearly to 41% B in A over 120 min (40 °C, flow rate of 300 nL/min). The positive ion spray voltage was 2,200 V. Orbitrap was used for primary MS with the following parameters: resolution = 120,000; quadrupole isolation; scan range = 200 to 1,400 *m/z*; radio frequency (RF) lens = 30%; automated gain control (AGC) target = 1×10^6; maximum injection time = 100 ms; 1 microscan. The acquisition of MS/MS spectra was performed in the Orbitrap (resolution = 30,000; quadrupole isolation; isolation window = 1.3 *m/z*; AGC target = 2×10^4; maximum injection time = 100 ms; 1 microscan) in a data-dependent manner: a precursor was excluded for 30 s if it was detected greater than three times within 30 s (mass tolerance: 10.00 ppm); peptides were selected by monoisotopic precursor selection; intensity threshold was 5×10^4; 2 to 10 charge states were selected; the precursor selection range was 200 to 1,400 *m/z*. The top 15 most intense precursors matching these criteria were subjected to subsequent fragmentation. Collision-induced dissociation (CID), higher-energy collisional dissociation (HCD), and electron-transfer/HCD (EThcD) were used for MS/MS acquisition. Precursors with charge states greater than two were subjected to all fragmentation modes; precursors with charge states of two were subjected to CID and HCD only. A collision energy of 30% was used for CID. A collision energy of 25% was used for HCD. A supplemental activation collision energy of 25% was used for EThcD.

Flow Cytometry. Cells were analyzed on a FACS Canto II flow cytometer or FACS Fortessa flow cytometer (BD Biosciences). Flow data were processed in

FlowJo (Tree Star). Cells (excluding erythrocytes) were stained with a fixable live/dead aqua zombie (BioLegend) for 15 min. The surface receptors were stained for 30 min on ice. For intracellular staining experiments, cells were fixed and permeabilized at this point using BD Cytofix/Cytoperm and then stained again. The following staining reagents were used: anti-CD45.2-BUV395 (BD Biosciences), anti-Thy1.1-PE (OT1 marker; BioLegend), anti-IFN-γ-AF488 (BioLegend), anti-CD8-APC (BioLegend), streptavidin-PE (BioLegend), GFP, DQLR-GFP, biotinylated DQLR-mPA, and biotinylated scrambled DQLR-mPA. At least 1,000,000 events were collected for each experimental replicate, except for binding experiments in which at least 1,000 gated events were collected.

Full-Length Protein Immunogenicity. For the DQLR-mPA versus PA experiment, 10 BALB/c mice per group (female, 6 to 8 wk old; Taconic) were anesthetized with isoflurane and administered 0.5 nmol of 0.2 μm–filtered protein in sterile PBS by retro-orbital injection on "protein" days. All mice were challenged with 0.1 nmol of wild-type PA on the "challenge" day. On bleed days, mice were bled via retro-orbital route (roughly 50 μL collected per bleed). Serum was collected and stored at −80 °C until enzyme-linked immunosorbent assay (ELISA) was performed.

For the DQLR-mPA versus PA versus DQLR + PA versus scrambled DQLR-mPA experiment, five BALB/c mice per group (female, 8 to 10 wk old; Taconic) were anesthetized by isoflurane and administered 0.5 nmol of 0.2 μm–filtered protein in sterile PBS by tail vein injection on "protein" days. On bleed days, mice were bled via submandibular routes (roughly 50 μL collected per bleed). Serum was collected and stored at −80 °C until ELISA was performed.

Anti-protein antibody titer was determined by ELISA. Medisorp 96-well plates (Thermo Fisher Scientific) were coated overnight at 4 °C with 10 μg/mL PA in PBS. Plates were washed with PBST (PBS with 0.1% Tween-20) and blocked with 5% fetal bovine serum (FBS) in PBS for 2 h at room temperature. Subsequently, plates were washed with PBST and incubated for 2 h at room temperature with serum dilutions including a control well which was not antigen coated. Plates were then washed and incubated with anti-mouse horseradish peroxidase (1:5,000 dilution in PBS; Thermo Fisher Scientific) and visualized with 1-Step Ultra-TMB (Thermo Fisher Scientific). The relative antibody titer was calculated as the highest dilution with greater than twice the $OD_{450\ nm}$ of the control well.

Peptide Immunogenicity. Peptides were tested for their ability to deplete $CD8^+$ T cells toward SIINFEKL and a proinflammatory T cell response using previously reported methods (2). Briefly, 300,000 OT1 $CD8^+$ T cells were administered intravenously (i.v.) via tail vein injection into 6- to 8-wk–old C57Bl6/J mice ($n = 4$ or 5 per group as shown; Taconic). A total of 60 μg peptide was then injected i.v. on days 1 and 6 retro-orbitally. On day 15, mice were challenged with an intradermal injection of OVA and LPS as previously described. On 19 d post-adoptive transfer, OT1 $CD8^+$ T cells from the peripheral blood were quantified as well as their activation by SIINFEKL by flow cytometry. On day 21, the inguinal lymph nodes were harvested, and OT1 $CD8^+$ T cells were quantified by flow cytometry.

Photoaffinity Labeling and Pull-Down. A total of 1 mL of packed mouse RBCs was treated with 40 mL of 5 mM sodium phosphate, pH 8.0, and centrifuged at 13,000 rpm (~20,000 *g*) to remove the hemoglobin (34). The ghost cells were incubated with either 1× PBS alone or DQLR peptides (1.0 μM in 1× PBS) on ice for 30 min. Ghost cells were then irradiated at 350 nM, 150 W for 30 min. Membrane portions were collected by centrifugation at 16,000 *g* for 5 min, after which the supernatant was discarded. Membranes were resuspended in 1 mL of 1× PBS and centrifuged again, after which the supernatant was discarded. This wash cycle was repeated two additional times. The streptavidin pull-down was performed by incubating the collected samples with 50 μL of Dynabeads MyOne Streptavidin T1 beads (catalog no.: 65602) for 20 min on ice followed by another incubation with 1 mL of 1× radioimmunoprecipitation assay buffer (Abcam, catalog no. ab156034) for 1 h at room temperature. The captured protein–peptide complex was eluted with 1× SDS loading buffer and then boiled for 10 min before analysis by SDS-PAGE.

Gel Band MS Analysis and Database Searching. Gel bands were excised, reduced with 5 mM DTT, alkylated with 10 mM iodoacetamide, and digested with trypsin at 37 °C as described previously (35). The dried peptide mix was reconstituted in a solution of 2% FA for MS analysis. Peptides were loaded with the autosampler directly onto a 50-cm EASY-Spray C18 column (ES803a, Thermo Fisher Scientific). Peptides were eluted from the column using a Dionex Ultimate 3000 Nano LC system with a 14.8-min gradient from 1% buffer B to 23% buffer B (100% acetonitrile, 0.1% FA), followed by a 0.2 min gradient to 80% buffer B, and held constant for 0.5 min. Finally, the gradient was changed from 80% buffer B to 99% buffer A (100% water, 0.1% FA) over 0.5 min and then held constant at 99% buffer A for 14 more minutes. The application of a 2.0-kV distal voltage electrosprayed the eluting peptides directly into the Thermo Exploris 480 mass spectrometer equipped with an EASY-Spray source (Thermo Fisher Scientific). Mass spectrometer–scanning functions and HPLC gradients were controlled by the Xcalibur data system (Thermo Fisher Scientific). The MS1 scan parameters were 60,000 resolution, AGC at 300%, and injection time (IT) at 25 ms. The MS2 scan parameters were 30,000 resolution, isolation width at 1.2, HCD collision energy at 28%, AGC target at 100%, and max IT at 55 ms. A total of 15 MS/MS scans were taken for each MS1 scan.

Tandem mass spectra were searched with Sequest (Thermo Fisher Scientific; version IseNode in Proteome Discoverer 2.5.0.400) against a mouse UniProt database (database version July 3, 2020; 55,585 entries containing common contaminants) with trypsin selected as the digestion enzyme. A fragment ion mass tolerance of 0.60 Da and a parent ion tolerance of 10.0 PPM were used. The carbamidomethyl of cysteine was specified in Sequest as a fixed modification. The oxidation of methionine was specified in Sequest as a variable modification. Scaffold (version Scaffold_4.11.1, Proteome Software, Inc.) was used to validate MS/MS-based peptide and protein identifications. Peptide identifications were accepted if they could be established at greater than 95.0% probability by the Percolator posterior error probability calculation (36). Protein identifications were accepted if they could be established at greater than 99.0% probability and contained at least two identified peptides. Protein probabilities were assigned by the ProteinProphet algorithm (37). Proteins that contained similar peptides and could not be differentiated based on MS/MS analysis alone were grouped to satisfy the principles of parsimony.

Bio-Layer Interferometry. In vitro–binding validation was performed using a ForteBio Octet RED96 system. Briefly, with the system set to 30 °C and 1,000 rpm, the streptavidin biosensor tips were dipped into 200 μL of 1.0 μM biotinylated peptide solution in kinetic buffer (KB) composed of 1× PBS, 0.1% bovine serum albumin, and 0.02% Tween-20. The tips loaded with peptides were then moved into wells containing various concentrations of recombinant Band 3 protein (Origene, catalog no. TP511222) in KB. Buffer-only and protein-only conditions (at the highest sampled protein concentration) were used as references for background subtraction. After a 180-s association step, the tips were dipped back into KB to obtain the dissociation curve. The association and dissociation curves were fitted with ForteBio Biosystems Data Analysis Software ($n = 5$, global fitting algorithm, binding model 1:1) to obtain dissociation constants (K_d). Similar experiments were performed against a control protein, anti-hemagglutinin antibody (12ca5).

Off-Target Cell Lines.

Cell culture. B16F10 and M-1 cells were purchased from American Type Culture Collection (ATCC CRL-6475 and ATCC CRL-2023, respectively). B16F10 were cultured in Dulbecco's Modified Eagle's Medium (DMEM) supplemented with 10% FBS, and M-1 were cultured in a 1:1 mixture of DMEM and Ham's F-12 medium with 2.5 mM L-glutamine adjusted to contain 15 mM Hepes, 0.5 mM sodium pyruvate, and 1.2 g/L sodium bicarbonate supplemented with 0.005 mM dexamethasone and 5% FBS. Both cell lines were maintained in an incubator under 37 °C and 5% CO_2 for at least three passages before experiment usage.

Human RBCs. Human erythrocytes were purchased from Zenbio (SER-10MLRBC). Blood was collected, processed, and tested by American Blood Bank Corp. in accordance with appropriate Food and Drug Administration regulations and guidance. The product was received cold, and a certificate of analysis was included.

Statistical Analysis. Statistical analysis and graphing was performed using Prism 8 (GraphPad). The listed replicates for each experiment indicate the number of distinct samples measured for a given assay. The significance for PA versus DQLR-mPA was determined using a one-way ANOVA with a Sidak's multiple comparisons test (****$P < 0.0001$). The significance for PA versus DQLR-mPA versus DQLR + PA versus scrambled DQLR-mPA was determined using a one-way ANOVA with a Dunnett's multiple comparisons test (*$P < 0.05$). The significance for the OT1 experiments was determined using Mann–Whitney *U* tests (*$P < 0.05$).

Ethical Compliance. All experiments described were performed in compliance with the Massachusetts Institute of Technology Committee on Animal Care (Institutional Animal Care and Use Committee).

Data Availability. All data needed to support the conclusions in the paper are present in the paper and *SI Appendix*.

CHEMISTRY

ACKNOWLEDGMENTS. Financial support for this work was provided by the Massachusetts Institute of Technology (MIT)/National Institute of General Medical Sciences Biotechnology Training Program (Grant T32 GM008334) to A.R.L. and A.J.Q. We thank the MIT Preclinical Modeling, Imaging, and Testing Core at the Koch Institute and in particular Aurora Connor for her insight and contributions; the MIT Division of Comparative Medicine and in particular Paul Chamberlain and Elizabeth Horrigan for their assistance with studies and training; the New England Regional Center of Excellence facility (Grant U54 AI057159) and Erica Gardner for PA expression; Arisa Shimada for the preparation of the peptide library reagent; Antonius Koller from the Biopolymers & Proteomics Core Facility at the Koch Institute for the gel band mass spectrometry analysis and database searching; Nina Hartrampf for assistance with automated peptide synthesis; and Nicholas Truex, Boyuan Wang, Chi Zhang, Sebastian Pomplun, Heemal Dhanjee, Ronald T. Raines, and Alex K. Shalek for support and helpful discussions.

1. N. Pishesha *et al*., Engineered erythrocytes covalently linked to antigenic peptides can protect against autoimmune disease. *Proc. Natl. Acad. Sci. U.S.A.* **114**, 3157–3162 (2017).
2. S. Kontos, I. C. Kourtis, K. Y. Dane, J. A. Hubbell, Engineering antigens for in situ erythrocyte binding induces T-cell deletion. *Proc. Natl. Acad. Sci. U.S.A.* **110**, E60–E68 (2013).
3. K. M. Lorentz, S. Kontos, G. Diaceri, H. Henry, J. A. Hubbell, Engineered binding to erythrocytes induces immunological tolerance to *E. coli* asparaginase. *Sci. Adv.* **1**, e1500112 (2015).
4. P. Serra, P. Santamaria, Antigen-specific therapeutic approaches for autoimmunity. *Nat. Biotechnol.* **37**, 238–251 (2019).
5. N. Svensen, J. G. A. Walton, M. Bradley, Peptides for cell-selective drug delivery. *Trends Pharmacol. Sci.* **33**, 186–192 (2012).
6. R. Liu, X. Li, W. Xiao, K. S. Lam, Tumor-targeting peptides from combinatorial libraries. *Adv. Drug Deliv. Rev.* **110–111**, 13–37 (2017).
7. L. M. Higgins *et al*., In vivo phage display to identify M cell-targeting ligands. *Pharm. Res.* **21**, 695–705 (2004).
8. Y. Ren *et al*., A d-peptide ligand of integrins for simultaneously targeting angiogenic blood vasculature and glioma cells. *Mol. Pharm.* **15**, 592–601 (2018).
9. M. Ying *et al*., Stabilized heptapeptide A7R for enhanced multifunctional liposome-based tumor-targeted drug delivery. *ACS Appl. Mater. Interfaces* **8**, 13232–13241 (2016).
10. X. Wei *et al*., A D-peptide ligand of nicotine acetylcholine receptors for brain-targeted drug delivery. *Angew. Chem. Int. Ed. Engl.* **54**, 3023–3027 (2015).
11. X. Wei *et al*., Retro-inverso isomer of Angiopep-2: A stable d-peptide ligand inspires brain-targeted drug delivery. *Mol. Pharm.* **11**, 3261–3268 (2014).
12. N. Yao *et al*., Discovery of targeting ligands for breast cancer cells using the one-bead one-compound combinatorial method. *J. Med. Chem.* **52**, 126–133 (2009).
13. L. Huang *et al*., Highly selective targeting of hepatic stellate cells for liver fibrosis treatment using a d-enantiomeric peptide ligand of Fn14 identified by mirror-image mRNA display. *Mol. Pharm.* **14**, 1742–1753 (2017).
14. T. N. M. Schumacher *et al*., Identification of D-peptide ligands through mirror-image phage display. *Science* **271**, 1854–1857 (1996).
15. D. M. Eckert, V. N. Malashkevich, L. H. Hong, P. A. Carr, P. S. Kim, Inhibiting HIV-1 entry: Discovery of D-peptide inhibitors that target the gp41 coiled-coil pocket. *Cell* **99**, 103–115 (1999).
16. B. P. Gray, K. C. Brown, Combinatorial peptide libraries: Mining for cell-binding peptides. *Chem. Rev.* **114**, 1020–1081 (2014).
17. B. A. Stoos, A. Náray-Fejes-Tóth, O. A. Carretero, S. Ito, G. Fejes-Tóth, Characterization of a mouse cortical collecting duct cell line. *Kidney Int.* **39**, 1168–1175 (1991).
18. F. C. Brosius III, S. L. Alper, A. M. Garcia, H. F. Lodish, The major kidney band 3 gene transcript predicts an amino-terminal truncated band 3 polypeptide. *J. Biol. Chem.* **264**, 7784–7787 (1989).
19. S. Liu *et al*., Solid tumor therapy by selectively targeting stromal endothelial cells. *Proc. Natl. Acad. Sci. U.S.A.* **113**, E4079–E4087 (2016).
20. A. R. Loftis *et al*., Anthrax protective antigen retargeted with single-chain variable fragments delivers enzymes to pancreatic cancer cells. *ChemBioChem* **21**, 2772–2776 (2020).
21. G. P. Gladstone, Immunity to anthrax: Protective antigen present in cell-free culture filtrates. *Br. J. Exp. Pathol.* **27**, 394–418 (1946).
22. J. A. Young, R. J. Collier, Anthrax toxin: Receptor binding, internalization, pore formation, and translocation. *Annu. Rev. Biochem.* **76**, 243–265 (2007).
23. N. Abboud, N. Casadevall, Immunogenicity of Bacillus anthracis protective antigen domains and efficacy of elicited antibody responses depend on host genetic background. *Clin. Vaccine Immunol.* **15**, 1115–1123 (2008).
24. A. T. Nishiya *et al*., Inhibitory effects of a reengineered anthrax toxin on canine oral mucosal melanomas. *Toxins (Basel)* **12**, 157 (2020).
25. S. Jack *et al*., A novel, safe, fast and efficient treatment for Her2-positive and negative bladder cancer utilizing an EGF-anthrax toxin chimera. *Int. J. Cancer* **146**, 449–460 (2020).
26. S. Kontos, J. A. Hubbell, Improving protein pharmacokinetics by engineering erythrocyte affinity. *Mol. Pharm.* **7**, 2141–2147 (2010).
27. E. A. Watkins *et al*., Persistent antigen exposure via the eryptotic pathway drives terminal T cell dysfunction. *Sci. Immunol.* **6**, eabe1801 (2021).
28. A. J. Quartararo *et al*., Ultra-large chemical libraries for the discovery of high-affinity peptide binders. *Nat. Commun.* **11**, 3183 (2020).
29. F. Touti, Z. P. Gates, A. Bandyopadhyay, G. Lautrette, B. L. Pentelute, In-solution enrichment identifies peptide inhibitors of protein-protein interactions. *Nat. Chem. Biol.* **15**, 410–418 (2019).
30. N. Hartrampf *et al*., Synthesis of proteins by automated flow chemistry. *Science* **368**, 980–987 (2020).
31. A. J. Mijalis *et al*., A fully automated flow-based approach for accelerated peptide synthesis. *Nat. Chem. Biol.* **13**, 464–466 (2017).
32. M. D. Simon *et al*., Rapid flow-based peptide synthesis. *ChemBioChem* **15**, 713–720 (2014).
33. I. Chen, B. M. Dorr, D. R. Liu, A general strategy for the evolution of bond-forming enzymes using yeast display. *Proc. Natl. Acad. Sci. U.S.A.* **108**, 11399–11404 (2011).
34. T. L. Steck, J. A. B. T.-M. Kant, Preparation of impermeable ghosts and inside-out vesicles from human erythrocyte membranes. *Methods Enzymol.* **31**, 172–180 (1974).
35. A. Shevchenko *et al*., Linking genome and proteome by mass spectrometry: Large-scale identification of yeast proteins from two dimensional gels. *Proc. Natl. Acad. Sci. U.S.A.* **93**, 14440–14445 (1996).
36. L. Käll, J. D. Storey, W. S. Noble, Non-parametric estimation of posterior error probabilities associated with peptides identified by tandem mass spectrometry. *Bioinformatics* **24**, i42–i48 (2008).
37. A. I. Nesvizhskii, A. Keller, E. Kolker, R. Aebersold, A statistical model for identifying proteins by tandem mass spectrometry. *Anal. Chem.* **75**, 4646–4658 (2003).